

MegBA: A High-Performance and Distributed Library for Large-Scale Bundle Adjustment

Jie Ren^{1,2*}, Wenteng Liang^{1*}, Ran Yan^{1†}, Luo Mai², Shiwen Liu¹, Xiao Liu¹

¹Megvii Inc.

²University of Edinburgh

Abstract

Large-scale Bundle Adjustment (BA) is the key for many 3D vision applications (e.g., Structure-from-Motion and SLAM). Though important, large-scale BA is still poorly supported by existing BA libraries (e.g., Ceres and g2o). These libraries under-utilise accelerators (i.e., GPUs), and they lack algorithms to distribute BA computation constrained by the memory on a single device.

In this paper, we propose MegBA, a high-performance and distributed library for large-scale BA. MegBA has a novel end-to-end vectorised BA algorithm that can fully exploit the massive parallel cores on GPUs, thus speeding up the entire BA computation. It also has a novel distributed BA algorithm that can automatically partition BA problems, and solve BA sub-problems using distributed GPUs. The GPUs synchronise intermediate solving state using network-efficient collective communication, and the synchronisation is designed to minimise communication cost. MegBA has a memory-efficient GPU runtime and exposes g2o-compatible APIs. Experiments show that MegBA can out-perform state-of-the-art BA libraries (i.e., Ceres and DeepLM) by up to 33x and 3.3x respectively, in public large-scale BA benchmarks. The code of MegBA is available at: <https://github.com/MegviiRobot/MegBA>.

1. Introduction

Bundle Adjustment (BA) is the key for many 3D vision applications [26, 41]. A BA problem needs to minimise the re-projection error between the camera poses and map points. The error is formulated as a non-linear square function, and it is minimised using iterative methods, such as Gauss-Newton (GN) [45], Levenberg-Marquardt (LM) [31] and Dog-Leg [37]. In each iteration, the BA algorithm differentiates the errors with respect to its states, and then constructs a linear system to be solved using algorithms, such

as Cholesky decomposition [9] and Precondition Conjugate Gradient (PCG) [14].

The wide adoption of city-level high-definition map for autonomous driving [8, 27, 28, 30] and indoor map for augmentation reality [36, 43, 48] has made large-scale BA an important yet challenging task in production. A production structure-from-motion application can produce a large number of images [6, 21], thus resulting in billions of points and observations to be applied with BA. Such a large-scale BA problem is orders of magnitude larger than those typically created by conventional computer vision applications [42, 49].

Solving a large-scale BA problem requires massive computation and memory resources. Such requirements go beyond the computational capacity and memory available on a single general-purpose processor (e.g., CPU). Practitioners are thus looking for BA libraries that can effectively exploit accelerators (e.g., GPU and TPU) and distribute BA computation to multiple devices [12, 16, 47].

Existing BA libraries (e.g., g2o [19], Ceres [5] and ADMM [7]), however, achieve insufficient performance in large-scale BA. We observe several reasons for this: (i) These systems under-utilise accelerators. Even though there are attempts, such as PBA [46] and g2o-GPU [4], to accelerate certain steps in BA, they fail to fully accelerate the entire BA computation, thus leaving key steps in BA (e.g., error differentiation and linear system construction) un-accelerated. (ii) Existing BA systems lack exact algorithms to distribute computation. Only until recently, there are efforts, such as RPBA [32], DPBA [12] and STBA [50], that propose *approximated* distributed BA algorithms. Though efficient, these algorithms require users to manually tune hyper-parameters that control the level of approximation [22], and they cannot guarantee convergence equivalent to a single device, making them difficult to be widely adopted in production.

In this paper, we propose MegBA, a high-performance and distributed library for large-scale BA. The design and implementation of MegBA make several contributions:

(1) Fully vectorised BA algorithm. We want to design

*Equal contribution, work conducted during internship at Megvii 3D

†Corresponding: yanran@megvii.com

a BA algorithm where all its expensive iterative operations can be *vectorised* as Single-Instruction-Multiple-Data (SIMD) [17] operations, thus enabling BA to fully exploit the massive parallel cores on accelerators. To achieve this design, we propose *JetVector*, a novel BA data structure that represents complex BA data as SIMD-aware vectors. JetVector can be efficiently processed by novel SIMD-aware BA kernels (e.g., matrix multiplication, inverse, inner project, etc.). These kernels achieve embarrassingly parallelism in completing *all* iteration-intensive operations in BA, thus achieving end-to-end acceleration.

(2) Exact distributed BA algorithm. We want to design an *exact* distributed BA algorithm which can distribute the solving of arbitrary BA problems to multiple devices without incurring any form of approximation. To this end, MegBA has a novel distributed BA algorithm which can *automatically* partition BA problems, and dispatches the sub-problems to distributed accelerators. The accelerators solve sub-problems using PCG in parallel, and synchronise intermediate PCG state using network-efficient collective communication (i.e., NCCL [23]). The synchronisation states are designed to minimise communication cost. MegBA can thus scale to many accelerators without incurring the convergence issues as in prior approximated BA systems.

(3) Memory-efficient engine and compatible APIs. We want to enable MegBA to run on as many as commodity GPUs and can be easily adopted by users of existing BA libraries. To achieve these goals, we implement an engine for MegBA where its memory usage is highly optimised on commodity GPUs (where GPU memories are not affluent). The APIs of MegBA are fully compatible with popular BA libraries: g2o and Ceres. Hence, many existing BA applications can benefit the substantial acceleration from MegBA with modest hardware and development costs.

We evaluate the performance of MegBA on cloud servers with up to 8 NVIDIA V100 GPUs. Experiments with large-scale BA benchmarks (i.e., Venice-1778 [6]) show that MegBA with 1 GPU can out-perform the de-facto BA library: Ceres (with 32 CPU cores) by 10x, showing the benefits of fully accelerating BA using GPUs. With 8 GPUs, MegBA out-performs Ceres by 35x, indicating the benefits for distributed BA computation. We further compare MegBA with DeepLM [22], a GPU-based fast BA library proposed very recently. MegBA out-performs DeepLM by 1.5x on a single GPU due to MegBA’s design of fully vectorising BA computation. With 8 GPUs, MegBA out-performs DeepLM by 3.4x, achieving the state-of-the-art result in large-scale BA.

2. Related Work

In this section, we describe the related work of MegBA. g2o [19] and Ceres [5] are **exact BA libraries** that can compute high-accuracy solutions to BA problems. These

libraries are originally designed for using multiple CPU cores, and they are ill-suited in using GPUs. Also, these libraries cannot support distributed execution, and they thus often suffer from out-of-memory errors in solving large-scale BA problems.

Many **approximated BA algorithms** have been proposed to speed up BA. PBA [46] addresses the performance issues; but the BA problems it can solve is heavily restricted by the memory capacity of a single device. \sqrt{BA} [13] proposed to replace Schur Complement with the memory-efficient nullspace projection of Jacobian, thus improving performance with single-precision float numbers. iSAM [25], iSAM2 [24], GTSAM [11], AprilSAM [44] exploit the influence of the states ordering. By contrast, ICE-BA [29] exploits the states in temporal orders. They solve BA incrementally by only linearising a few states each time for high efficiency.

Though efficient, approximated BA algorithms modify the original BA problems to improve hardware efficiency. However, they adversely affect convergence and are thus not widely used in production. As a result, much commercial 3D vision software, such as ContextCapture [1], PIX4D [3], and Terra [2] favour exact BA libraries, and supporting exact distributed BA computation thus becomes a key design goal of MegBA.

The need for large-scale BA has motivated **distributed BA systems** to be designed recently. RPBA [32], DPBA [12], STBA [50] partition the BA problems based on an ADMM. These ADMM-based systems suffer from excessive redundant computation on distributed devices, making them even under-perform single-node systems. Further, their users need to manually partition BA problems, and the optimal partitioning is hard to approach by manual tuning. BA-Net [40] and DeepLM [22] leverages GPU to speed up BA. They however rely on PyTorch to use GPU, which incurs non-trivial overheads of manipulating GPU and excessive memory copies, making GPU under-utilised.

Task-specific hardware and knowledge are also used for accelerating BA. GBP [35] uses a neural processing unit (i.e., GraphCore IPU) to speed up BA, and the limited availability of IPU makes GBP difficult to be served as a widely adopted solution. Practitioners also propose an approximated BA solver tailored for facial capture [18], and this solver cannot be used for arbitrary BA problems such as structure-from-motion.

3. Preliminaries

In this section we introduce the preliminaries of MegBA design. A BA problem can be represented as a graph and formulated as the minimisation of a non-linear square error objective function:

$$\mathbf{x}^* = \arg \min_{\mathbf{x}} \sum e_{i,j}^\top \Sigma_{i,j} \mathbf{e} \mathbf{x}_{i,j}, \quad (1)$$

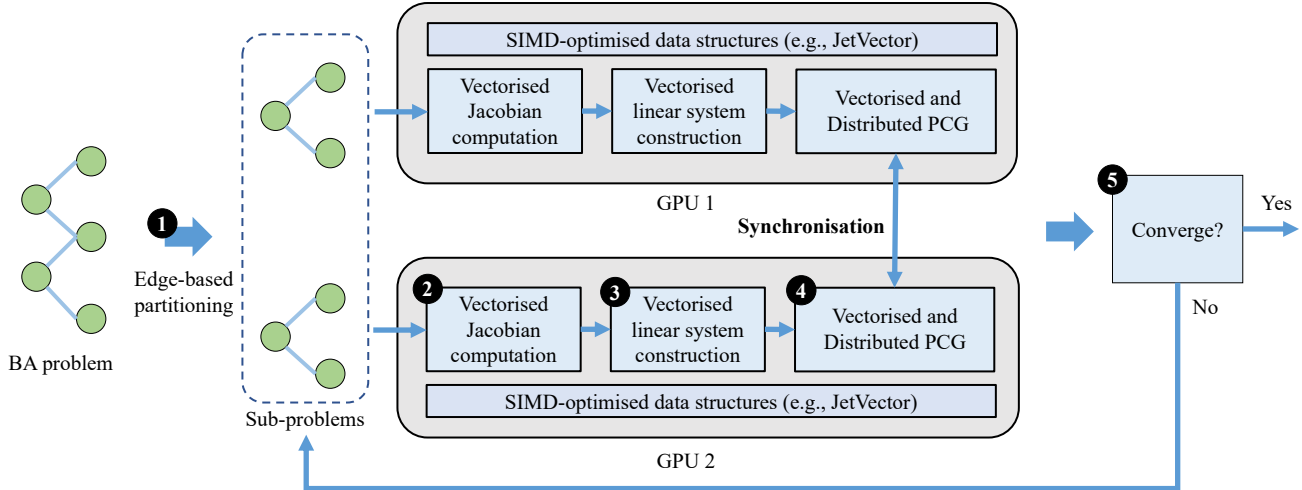


Figure 1. **MegBA overview.** (1) MegBA partitions a BA problem based on edge. BA sub-problems are in the same size, and they are dispatched to distributed GPUs. On each GPU, (2) Jacobians are computed with vectorised operations; (3) linear system constructed with vectorised operations, and (4) vectorised and distributed PCG algorithm is applied to solve the linear system, and intermediate PCG states are synchronised using collective communication. Step (2), (3) and (4) are executed iteratively until (5) convergence criteria has been met.

where $e_{i,j}$ is the constraint (i.e. error or graph edge) between state (i.e. parameter or graph node) x_i and x_j , $\Sigma_{i,j}$ is the information matrix.

Solving Equation 1 is equivalent to iteratively updating the incremental amount Δx , given by the linear system $H\Delta x = g$, upon the current state x until convergence. Here, the Hessian matrix $H = J^T \Sigma J$ for GN method and $H = J^T \Sigma J + \lambda I$ for LM method, the residual vector g equals to $-J^T \Sigma r$, J is the Jacobian of the error e with respect to current state x . Hessian is often stored as Compressed Sparse Row (CSR) [15], represented by VAL, COLIND and ROWPTR vectors. VAL and COLIND are in $O(n)$ space, where n is the dimension of state. ROWPTR is in $O(|R|)$, where $|R|$ is the number of rows.

To solve BA problems with special structure, BA libraries often leverage Schur Complement (SC) in the following way:

$$\begin{bmatrix} B & E \\ E^T & C \end{bmatrix} \begin{bmatrix} \Delta x_c \\ \Delta x_p \end{bmatrix} = \begin{bmatrix} v \\ w \end{bmatrix} \quad (2)$$

where B and C are block diagonal and they are related to camera-camera and point-point edges, respectively. E refers to edges between camera and point. v and w refer to the residual vectors for camera and point states.

Solving $H\Delta x = g$ is equivalent to compute the incremental update for states related to cameras Δx_c by solving an alternative linear system, often called Reduced Camera System (RCS)

$$[B - EC^{-1}E^T]\Delta x_c = v - EC^{-1}w, \quad (3)$$

and followed by a substitution Δx_c into

$$\Delta x_p = C^{-1} (w - E^T \Delta x_c), \quad (4)$$

to get the update for 3D map points.

BA libraries often solve linear systems using either direct methods or iterative methods. On the one hand, direct methods, such as Gaussian-Elimination, LU, QR, and Cholesky Decomposition, return optimised solution of x in one pass. They however suffer from $O(n^3)$ time and $O(n^2)$ space complexity, making them only suitable for small-scale BA problems. On the other hand, iterative methods, such as PCG [41], are suitable for large-scale BA problems. Specifically, Iterative Linear Solver PCG [6] replaces the explicit computation of $EC^{-1}E^T$ with multiple iterative sparse matrix-vector operations. It reduces the space complexity to $O(n)$, thus saving memory.

4. MegBA Design

This section introduces the design of MegBA. The design goals of MegBA are two-fold: (i) fully exploiting accelerators and (ii) having algorithms that can effectively distribute BA computation in the exact form.

Figure 1 presents an overview of how MegBA achieves these goals. A MegBA user declares a BA problem which is represented as a graph with nodes and edges. MegBA can automatically partition the BA problem based on edges with the aim of each BA sub-problem having an even number of edges, leading to balanced sub-problem solving workloads (1). On each GPU, the BA computation is fully vectorised and thus can achieve full SIMD operation. Specifically, each GPU first (2) computes the Jacobian (i.e. differentiation of the edge for the node), and then (3) construct the linear system by computing the Hessian matrix H and constant vector g , and finally, (4) apply PCG to compute the update for adjusting the current BA sub-problem. The

Algorithm 1 SIMD-optimised Vectorised BA

- 1: Given a BA Problem with initial state \mathbf{x} .
 - 2: Partition Hessian \mathbf{H} into $\mathbf{B}, \mathbf{C}, \mathbf{E}, \mathbf{E}^T$ based on Schur Complement (Equation 2).
 - 3: Initialise *JetVectors* on accelerators.
 - 4: **while** BA Convergence Criteria not satisfied **do**
 - 5: Compute Output \mathbf{r} and Jacobian \mathbf{J} with respect to the state \mathbf{x} ; /* SIMD */
 - 6: Construct $\mathbf{B}, \mathbf{C}, \mathbf{E}, \mathbf{E}^T$ by computing $\mathbf{J}^T \mathbf{J}$ and the residual \mathbf{g} by $-\mathbf{J}^T \mathbf{r}$; /* SIMD */
 - 7: Given $\mathbf{B}, \mathbf{C}, \mathbf{E}, \mathbf{E}^T, \mathbf{x}$ as \mathbf{x}^0 , run PCG (Algorithm 2) to obtain $\Delta \mathbf{x}_c$; /* SIMD */
 - 8: Substitute $\Delta \mathbf{x}_c$ into Equation 4, and then run $\Delta \mathbf{x}_p = \text{spmv}(\text{inv}(\mathbf{C}), \text{sub}(\mathbf{w}, \text{spmv}(\mathbf{E}^T, \Delta \mathbf{x}_c)))$; /* SIMD */
 - 9: Update \mathbf{x} .
 - 10: **end while**
-

PCG intermediate state is synchronised, so that MegBA can eventually solve the shared global BA problem. The BA update step is iteratively performed until a user-defined convergence criterion is met (5).

In the following, we will describe how do we achieve end-to-end vectorisation in BA computation, and how do we design an exact distributed BA computation.

4.1. SIMD-optimised Vectorised BA

Modern accelerators and processors often support SIMD operations to fully exploits their massive parallel cores. Though promising, SIMD is particularly challenging to implement for BA. It will require us to (i) vectorise all iteration-intensive BA operations, so that they can be executed in the SIMD manner, and (ii) implement BA's memory-intensive input, state and output in SIMD-based data structures, thus minimising the costs of memory allocation and movement within accelerators.

Algorithm 1 shows the SIMD-optimised fully vectorised BA designed in MegBA. This algorithm is given a BA problem with an initial state (Line 1). It partitions the Hessian based on Schur Complement (Line 2). Before starting BA, MegBA will initialise **JetVector** (Line 3), a novel data structure to represent BA data in a SIMD-based format. Compared to conventional BA data structure: *Jet* implemented in Ceres, *JetVector* represents a list of Jets (i.e., Array-of-Structure) as a single data object where *Jet*'s data fields: *data* and *grad* across all items are represented as single arrays (i.e., Array-within-Structure). The same transformation is applied to other memory-intensive BA data structures where their details are omitted due to page limits.

In each BA iteration (Line 4-10), Algorithm 1 first applies SIMD to accelerate the Jacobian computation (Line 5). To support differentiation computation towards arbitrary

Algorithm 2 SIMD-optimised Vectorised PCG

- 1: Given initial state \mathbf{x}^0 , and $\mathbf{B}, \mathbf{C}, \mathbf{E}, \mathbf{E}^T, \mathbf{v}, \mathbf{w}$ from Schur Complement.
 - 2: $\mathbf{r}^0 = \text{sub}(\mathbf{b}, \mathbf{A}\mathbf{x}^0)$; /* SIMD */
 where $\mathbf{A}\mathbf{x}^0 = \text{sub}(\text{spmv}(\mathbf{B}, \mathbf{x}^0), (\mathbf{E}, \text{spmv}(\text{inv}(\mathbf{C}), \text{spmv}(\mathbf{E}^T, \mathbf{x}^0))))$, and
 $\mathbf{b} = \text{sub}(\mathbf{v}, \text{spmv}(\mathbf{E}, \text{spmv}(\text{inv}(\mathbf{C}), \mathbf{w})))$
 - 3: $n = 0$
 - 4: **while** Convergence Criteria not satisfied **do**
 - 5: $\mathbf{z}^n = \text{spmv}(\mathbf{B}, \mathbf{r}^n)$; /* SIMD */
 - 6: $\rho^n = \text{dotproduct}(\mathbf{r}^n, \mathbf{z}^n)$; /* SIMD */
 - 7: **if** $n > 1$ **then**
 - 8: $\beta^n = \rho^n / \rho^{n-1}$
 - 9: $\mathbf{p}^n = \text{add}(\mathbf{z}^n, \beta^n \mathbf{p}^{n-1})$; /* SIMD */
 - 10: **else**
 - 11: $\mathbf{p}^n = \mathbf{z}^n$; /* SIMD */
 - 12: **end if**
 - 13: $\mathbf{q}^n = \mathbf{A}\mathbf{p}^n$; /* SIMD */
 where $\mathbf{A}\mathbf{q}^n = \text{sub}(\text{spmv}(\mathbf{B}, \mathbf{q}^n), (\mathbf{E}, \text{spmv}(\text{inv}(\mathbf{C}), \text{spmv}(\mathbf{E}^T, \mathbf{q}^n))))$
 - 14: $\alpha^n = \text{div}(\rho^n, \text{dotproduct}(\mathbf{p}^n, \mathbf{q}^n))$ /* SIMD */
 - 15: $\mathbf{x}^{n+1} = \text{add}(\mathbf{x}^n, \alpha^n \mathbf{p}^n)$; /* SIMD */
 - 16: $\mathbf{r}^{n+1} = \text{sub}(\mathbf{r}^n, \alpha^n \mathbf{q}^{n-1})$; /* SIMD */
 - 17: $n = n + 1$
 - 18: **end while**
-

BA problems, we implement a set of SIMD automatic differentiation kernels, including basic arithmetic operators (i.e. addition, subtraction, multiplication, division), trigonometry, and the conversion between quaternion and rotation matrix, thus making the Jacobian computation accelerated in most, if not all, BA problems we have in production. Line 6-7 further computes the product of the Jacobian and the residual with SIMD operations. The results are passed to a carefully designed PCG which is later described in Algorithm 2. The solving results are returned by the PCG and we eventually update the state of the BA problem using SIMD operations (Line 8-9).

SIMD-optimised vectorised PCG. Given its focus on large-scale BA problems, MegBA adopts the memory-efficient iterative PCG as the default linear system solver. To accelerate iterative PCG, we design SIMD-optimised vectorised PCG shown in Algorithm 2. In this algorithm, all computation-intensive operations working on vectors and matrix (Line 2, 5, 6, 9, 11, 13, 14-16) are implemented using a set of SIMD operations (e.g., *spmv* and *dotproduct*) designed in MegBA. This allows MegBA to achieve end-to-end vectorisation within iterative PCG.

4.2. Exact Distributed BA

We then describe how to distribute the vectorised BA computation to distributed SIMD devices. The distributed

BA computation has two main benefits: (i) it can consolidate the memories on distributed devices, thus providing tremendous memory for large-scale BA; (ii) it can also combine the computational power on multiple devices, thus making large-scale BA faster than a single device. Though beneficial, distributed BA computation is challenging to design. Many early efforts have dived into the direction of designing approximated distributed BA, but the approximation can hurt BA convergence.

In this section, we take *preserving the exactness of a BA problem* as the paramount goal when designing MegBA's distributed BA algorithm. At the high level, the MegBA distributed BA algorithm has two major components: (i) a method that can divide a BA problem into sub-problems which can be solved by parallel vectorised PCGs, and (ii) an algorithm that can synchronise the states of the parallel PCGs so that these algorithms can collectively solve the original global BA problem.

4.2.1 Edge-based partitioning of BA problems

We want to come up with a generic method to partition a BA problem, and each parallel device is assigned with a sub-problem of the equal size. Our partitioning method is based on a generic observation of BA problems: the complexity of solving a BA problem is mainly decided by the number of edges. To distribute the solving workload, we can partition the problem based on edges, without introducing any form of approximation.

Given a BA problem, we first consider partitioning its Jacobian \mathbf{J} whose row index corresponds to the edge number, into several blocks horizontally:

$$\mathbf{J} = [\mathbf{J}_1 \quad \mathbf{J}_2 \quad \dots \quad \mathbf{J}_i]^T. \quad (5)$$

Assuming identity information matrix is given here, Hessian \mathbf{H} can be partitioned:

$$\mathbf{H} = \mathbf{J}^T \mathbf{J} = \sum_{i=1}^N \mathbf{J}_i^T \mathbf{J}_i = \sum_{i=1}^N \mathbf{H}_i. \quad (6)$$

In Schur Complement, each \mathbf{H}_i can be thus represented as sub-blocks:

$$\mathbf{H}_i = \begin{bmatrix} \mathbf{B}_i & \mathbf{E}_i \\ \mathbf{E}_i^T & \mathbf{C}_i \end{bmatrix}. \quad (7)$$

Note that we have $\mathbf{J}_1 \mathbf{J}_2 \dots \mathbf{J}_i \mathbf{B} = \sum_{i=1}^N \mathbf{B}_i$, $\mathbf{E} = \sum_{i=1}^N \mathbf{E}_i$, $\mathbf{E}^T = \sum_{i=1}^N \mathbf{E}_i^T$, and $\mathbf{C} = \sum_{i=1}^N \mathbf{C}_i$. The number of non-zero parameter blocks in \mathbf{E} or \mathbf{E}^T equals to the number of edges in the problem. Notably, the sub-matrices \mathbf{B}_i and \mathbf{C}_i (block-diagonal) have the same number of non-zero elements as \mathbf{B} and \mathbf{C} , respectively.

Despite that matrices are in the CSR format, \mathbf{E} and \mathbf{E}^T still require massive memory, especially in large-scale BA. Whereas the number of non-zero elements in \mathbf{E}_i and \mathbf{E}_i^T are much less than \mathbf{E} and \mathbf{E}^T . Given this observation, we then propose to *divide* the matrix \mathbf{E} and \mathbf{E}^T and dispatches their partitions onto multiple devices. Each device can account for an even number of edges, and they *complete* expensive matrix and vector computation in a fully asynchronous manner.

4.2.2 Synchronising distributed BA states

The distributed devices are solving their sub-problems in parallel, and we must synchronise their solving states so that we eventually solve the original global BA problem. There are two important distributed BA states to synchronise:

(i) Synchronising distributed linear systems. Linear systems are independently constructed on devices (Line 6 in the Algorithm 1), and we want to ensure these linear systems are synchronised. Specifically, to calculate the output r and the Jacobian J for each edge. The VAL of \mathbf{B} , \mathbf{C} , \mathbf{E}_i and \mathbf{E}_i^T are calculated as $J^T J$. The VAL of \mathbf{B} and \mathbf{C} are then synchronized on each device using a distributed summation operation (i.e., all-reduce in MPI). The residual g is figured out by $-J^T r$.

(ii) Synchronising distributed PCG algorithms. The PCG algorithms run independently on parallel devices, and we want to ensure they are converging to the same optimal solution. To guarantee this, we want to transform the Algorithm 2 into an equivalent distributed version (i.e., exact transformation). This transformation is based on a key observation that: in the Algorithm 2, the computation of $\mathbf{A}\mathbf{x} = [\mathbf{B} - \mathbf{E}\mathbf{C}^{-1}\mathbf{E}^T]\mathbf{x}$ involved in the Line 2 and 13 are both memory and computation intensive. We thus consider to distribute its computation to multiple devices.

We show how the distributed PCG is implemented in Algorithm 3. For simplicity, the declaration of this distributed algorithm follows the widely adopted MapReduce style [10]. In this algorithm, we adopt the edge-based partition method to decompose the gigantic $\mathbf{A}\mathbf{x}$ (Line 1), and the sub-computation is mapped to multiple devices (Line 2). All devices compute their local solving results asynchronously (Line 3) and then use an MPI-style all-reduce operation to synchronise the γ in PCG. The devices then proceed in their local solving process (Line 5-6) and then compute the synchronised state using an all-reduce again (Line 7). The final solving results are thus consistent on all devices (Line 8).

5. MegBA Implementation

This section describes the implementation of MegBA. MegBA is written in CUDA C and C++, and its full implementation contains 17,606 Line-of-Code (LoC).

Algorithm 3 Distributed PCG

- 1: Known $Ax = [B - EC^{-1}E^T]x$, $E = \sum_i E_i$.
 - 2: Map B , C , v , w , x and E_i onto device i .
 - 3: Asynchronously compute $\tau_i = E_i^T x$ on device i .
 - 4: Reduce $\gamma = \sum \tau_i$ and synchronise γ onto device i .
 - 5: Asynchronously compute $\eta = C^{-1}\gamma$.
 - 6: Asynchronously compute $\iota_i = E_i\eta$.
 - 7: Reduce $\kappa = \sum \iota_i$.
 - 8: finally $Bx + \kappa$.
-

We keep two goals in mind when implementing MegBA: (i) We want to optimise the memory efficiency of MegBA, thus allowing large-scale BA to be completed with memory-constrained commodity GPUs; (ii) We want to implement the APIs of MegBA that are fully compatible with existing BA libraries: g2o and Ceres, making it easy to port existing BA applications to MegBA. In the following, we highlight how MegBA implementation achieves these goals. The description of the full MegBA implementation can resort to the documents of our library.

5.1. Memory-efficient GPU Engine

We implement MegBA on Nvidia GPUs, and our implementation optimises memory efficiency based on two techniques:

(i) Predicting BA memory buffer usages to minimise memory allocation. Allocating GPU memories is expensive and it can block GPU operators, thus decreasing GPU utilisation. To minimise memory allocation, we leverage a key observation specific to BA computation: The automatic differentiation works on GPU buffers that are in the same size across BA iterations. By monitoring the sizes of GPU buffers used in the forward pass of differentiating the BA errors, we can predict the sizes of all memory buffers involved in future BA iterations. Based on this observation, we can thus pre-allocate these memory buffers in a memory pool, and thus avoiding calling CUDA driver to allocate memory during runtime.

(ii) Sharing memories among GPU threads. MegBA will launch many GPU threads to maximise the level of parallelism. Each GPU thread has dedicated memory. To minimise the memory footprint, we achieve effective sharing of memory among GPU threads. This sharing is possible based on a key observation for BA computation. In a BA problem, assuming that the dimension of each camera state and each point state is a and b , respectively, we can execute $a + b$ GPU threads to process the data J_i and r_i of the i^{th} Edge to calculate H and g of the linear system. Since each Edge accounts for B , C , E , E^T in the H , we let the first a threads in charge of the calculations of B and E , and the last b threads for C and E^T . During this process, J_i is frequently visited, we initialized $(a + b) * \text{sizeof}(\text{dtype})$ shared

Dataset	#Points	#Observations
Trafalgar-257	65132	225911
Ladybug-1723	156502	678718
Dubrovnik-356	226730	1255268
Venice-1778	993923	5001946
Final-13682	4456117	28987644

Table 1. Dataset Statistics.

memory for these $a + b$ threads, and each thread caches a piece of J_i (the size of J_i is equal to $a + b$). The $a + b$ threads can thus freely load J_i from the shared memory.

To make memory sharing effective, MegBA achieves both *coalesced loading* and *the elimination of wrap divergence*. Specifically, the thread block is configured to be $(32, a + b)$ and a total number of $(\#Edges/32)$ thread blocks are initiated. The reason why using 32 for the thread block x dimension is that it can first be read coalesced from JetVector, and write to shared memory in a coalesce manner.

Meanwhile, the first a threads and the last b threads execute different kernels. Making the thread block y dimension be $a + b$ effectively avoid wrap divergence.

5.2. Compatible and Extensible APIs

We implement the APIs of MegBA in a way that is fully compatible with g2o and Ceres. The MegBA APIs contain two major components:

(i) Declaring BA problems. Following the API convention of g2o and Ceres, a BA problem in MegBA is declared a graph that contains nodes and edges. The MegBA nodes describe the 3D coordinates or the poses of cameras and these nodes can be directly imported from g2o and Ceres applications. The MegBA edges are error functions that can be written using the Eigen library [20], identical to Ceres. A MegBA user can build a large BA problem by adding BA nodes and edges (using the g2o-equivalent *AddEdge* and *AddNode* functions).

(ii) Choosing BA solvers. MegBA also support users to choose solvers given the characteristics of their BA problems. The default solver is the SIMD-optimised distributed PCG which can automatically use multiple GPUs. Given a small-scale BA problem where intrinsic parallelism is not sufficient, MegBA provides users with the CPU-optimised CHOLMOD solver [9]. In MegBA, a solver is switchable (e.g., CuSparsar [34] or CuSolver [33]), and it can be extended to solve generic graph optimisation problems as in g2o.

6. Experimental Evaluation

For evaluation, we use the BA datasets provided by BAL [6]. We choose 5 BAL datasets: Trafalgar-257, Ladybug-1723, Dubrovnik-356, Final-13682 and Venice-1778. These datasets contain varied numbers of points and

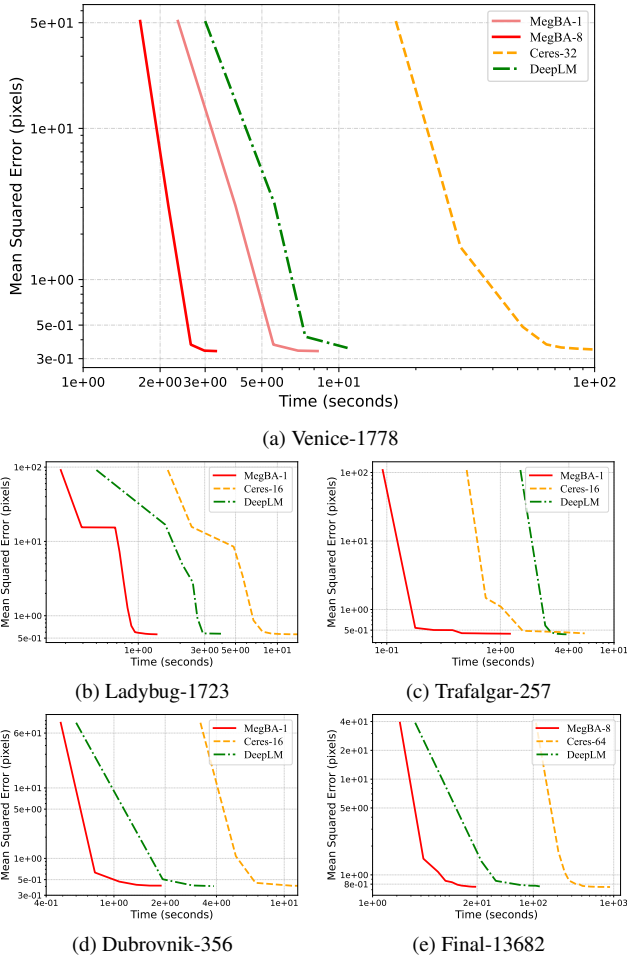


Figure 2. **Overall performance.** *MegBA-X* refers to using X used GPUs, *Ceres-X* refers to using X CPU threads.

observations, and their statistics are listed in Table 1. We use the accuracy-friendly 64-bit floating points (FP64) as the default data format, unless otherwise specified.

We compare MegBA with two baselines: (i) Ceres [5] (version 2.0) is the most popular BA library that can efficiently use massive CPU cores, and (ii) DeepLM [22] is the state-of-the-art GPU-based BA library (2021), and it was shown to out-perform other popular BA libraries: STBA [50] and PBA [46]. The PyTorch version is 1.19 in DeepLM.

All experiments run on a cloud server that has 80 Intel Xeon 2.5GHz CPU cores, 8 Nvidia V100 GPUs and 320GB memory. The GPUs are inter-connected using NVLink 2.0.

6.1. Overall Performance

We first evaluate the overall performance of MegBA, Ceres and DeepLM. Since MegBA and Ceres can both use parallel processors, we try different processor configura-

tions and report their best results only. MegBA uses from 1 to 8 GPUs, and Ceres uses from 1 to 80 CPU threads. We measure the Mean Squared Error (MSE) in pixels over time, and the BA terminates when the target $\|\Delta\mathbf{x}\|_2 \leq \epsilon \|\mathbf{x}\|_2$ has been reached, where $\epsilon = 1e^{-8}$.

Figure 2 shows the evaluation results. In the Venice-1778 dataset (Figure 2(a)), MegBA achieves the best performance with 8 GPUs, Ceres achieves the best performance with 32 CPU threads (i.e., giving more CPU threads to Ceres does not further improve its performance), while DeepLM can only use a single GPU. MegBA completes with 3.302 seconds while Ceres uses 111 seconds, showing the substantial speed-up (33x), which indicates the benefits of fully exploiting GPUs to accelerate BA computation. For GPU-based BA libraries, MegBA can complete with 8.254 seconds while DeepLM spent 10.8 seconds, showing the effectiveness of implementing full vectorisation for BA on a single GPU. With more GPUs, MegBA out-performs DeepLM by 3.3x, which reflects the necessity of adopting multiple GPUs.

Thanks to the vectorisation and distributed BA designs, MegBA becomes the state-of-the-art in the large BA dataset (i.e., Final-13682). As shown in Figure 2(e), MegBA completes in 18.9 seconds, while DeepLM uses 120.3 seconds (6.4x speed-up) and Ceres even uses 901 seconds (47.6x speed-up). In other datasets (Figure 2(b)-(d)), we observe similar speed-up achieved by MegBA, indicating the general effectiveness of our proposed approaches. We omit the discussion of these datasets, and their results are reported in Table 2.

6.2. Scalability

Table 3 further provides the detailed experimental results to show the scalability of MegBA, Ceres and DeepLM. In the Venice-1778 dataset, Ceres can consistently reduce the BA time from 162 seconds to 111 seconds. However, with 64 CPU threads, its performance drops. MegBA, on the other hand, can consistently improve its performance by adding GPUs (from 8.254 seconds to 3.302 seconds if we increase the number of GPUs from 1 to 8). In addition, the large dataset (Final-13682) can better show the scalability of MegBA. By increasing the number of GPUs from 4 to 8, MegBA can reduce the time from 23.8 seconds to 18.9 seconds, while Ceres can only reduce from 2040 seconds to 901 seconds using 64 CPU threads.

6.3. Floating point precision

The accuracy of solving a BA problem is sensitive to the choice of floating point precision (i.e., 32-bit vs. 64-bit floating points). We further evaluate MegBA in all datasets with 32-bit and 64-bit floating points, and we report the results of Venice-1778 and Final-13682 in Table 4. Other datasets show consistent results and we omit them

	Trafalgar-257			Ladybug-1723			Dubrovnik-356		
	MSE	Time	Mem	MSE	Time	Mem	MSE	Time	Mem
Ceres-1	0.448	5.77	0.19	0.563	62.9	0.53	0.393	132.0	0.11
Ceres-8	0.449	5.91	0.19	0.562	39.4	0.53	0.393	122.0	0.11
Ceres-16	0.448	5.52	0.19	0.562	34.5	0.53	0.393	116.0	0.11
Ceres-32	0.449	5.66	0.19	0.562	36.7	0.53	0.393	123.0	0.11
Ceres-64	0.448	5.70	0.19	0.562	40.5	0.53	0.393	125.0	0.11
DeepLM	0.434	3.82	0.018	0.573	3.93	0.048	0.404	3.86	0.07
MegBA-1	0.440	1.28	1.3	0.561	1.35	2.6	0.410	1.68	4.2

Table 2. **Performance of MegBA, Ceres and DeepLM in Trafalgar-257, Ladybug-1723 and Dubrovnik-356.** These datasets are small and thus MegBA does not need more than 1 GPU. We only report MegBA-1 here. MSE is the final Mean Squared Error (pixels), Time is in BA duration, and Mem is the memory cost in GB.

	Venice-1778			Final-13682		
	MSE	Time	Mem	MSE	Time	Mem
Ceres-1	0.341	162	0.56	0.746	2040	2.89
Ceres-8	0.341	129	0.56	0.746	1090	2.89
Ceres-16	0.341	116	0.56	0.746	949	2.89
Ceres-32	0.341	111	0.56	0.746	930	2.89
Ceres-64	0.341	125	0.56	0.746	901	2.89
DeepLM	0.352	10.8	0.29	0.758	120.3	1.31
MegBA-1	0.336	8.254	14.9	OOM	OOM	OOM
MegBA-2	0.336	5.427	15.8	OOM	OOM	OOM
MegBA-4	0.336	4.016	18.6	0.751	23.8	88
MegBA-8	0.336	3.302	23.2	0.751	18.9	96

Table 3. **Scalability.** MegBA- X refers to MegBA with X GPUs and Ceres- X refers to Ceres with X CPU threads.

	Venice-1778			Final-13682		
	MSE	Time	Mem	MSE	Time	Mem
MegBA-1(FP32)	0.337	2.080	8.3	OOM	OOM	OOM
MegBA-1(FP64)	0.336	8.254	14.9	OOM	OOM	OOM
MegBA-2(FP32)	0.337	1.863	9	OOM	OOM	OOM
MegBA-2(FP64)	0.336	5.427	15.8	OOM	OOM	OOM
MegBA-4(FP32)	0.337	1.734	11.6	0.751	3.9	48
MegBA-4(FP64)	0.336	4.016	18.6	0.751	23.8	88
MegBA-8(FP32)	0.337	2.118	16	0.755	3.8	56
MegBA-8(FP64)	0.336	3.302	23.2	0.751	18.9	96

Table 4. **Performance with 32-bit and 64-bit floating points.** MegBA- X refers to test MegBA with X GPUs in FP32 or FP64 precision. OOM refers to out-of-memory.

here. In the dataset of Final-13682, with 4 GPUs, MegBA (FP32) can complete in 3.9 seconds and MegBA (FP64) can complete in 23.8 seconds, while both of them are reaching the same MSE. This shows that the exactness of the distributed BA algorithm in MegBA. Even with lower precision, MegBA can reach the same MSE as double precision; but offering 6.1x speed up, making MegBA (FP32) be the state-of-the-art in Final-13682.

7. Limitations

Though promising, MegBA still have the following limitations: (i) *Memory footprint.* Even though MegBA has a memory-efficient engine, its pursuit for solving exact BA problems when distributing computation makes it consume substantial memory, compared to GPU-based BA algorithm: DeepLM. We will continue to investigate how to improve the memory efficiency of MegBA. For example, replacing the Hessian in BA with memory-saving implicit Hessian. (ii) *Hardware dependency.* Even though the design of MegBA is general (i.e., SIMD and distributed computation), the current implementation of MegBA is limited on Nvidia GPUs, leaving other SIMD-enabled processors, such as ARM Neon and AMD ATI, un-supported. We will investigate how to support more hardware platforms in MegBA. (iii) *Lack of analytical differentiation support.* MegBA aims to be a general solution for BA problems, and as a result, it supports automatic differentiation as the first step, which allows users to provide any error functions. However, it does not support analytical differentiated function, limiting MegBA to further improve its performance. We will address this limitation in the future.

8. Conclusion

In this paper, we present MegBA, a novel high-performance and distributed BA library that makes large-scale BA efficient. MegBA has novel designs that can fully accelerate BA computation on a single GPU, and it can exploit multiple GPUs without compromising BA accuracy. MegBA is implemented on general-purpose GPUs and it exposes compatible and extensible APIs, making MegBA easy to be adopted in production. Experimental results show that MegBA can achieve up to 33x and 3.3x performance improvement over state-of-the-art BA libraries, showing the promises of the proposed designs.

References

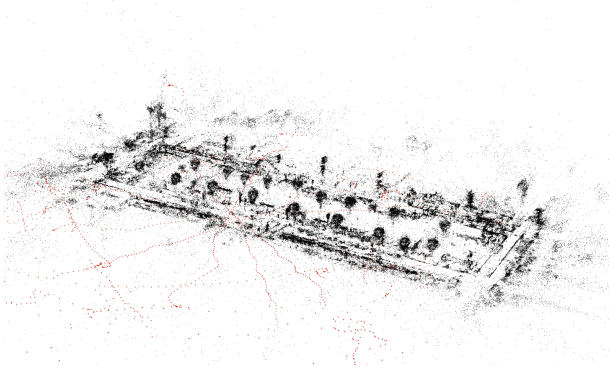
- [1] Contextcapture: 4d digital context for digital twins. <https://www.bentley.com/en/products/brands/contextcapture>. 2
- [2] Dji terra. <https://www.dji.com/cn/dji-terra>. 2
- [3] Pix4d. <https://www.pix4d.com/>, 2011. 2
- [4] adaskit Team. A cuda implementation of bundle adjustment. <https://github.com/fixstars/cuda-bundle-adjustment>, 2020. 1
- [5] Sameer Agarwal, Keir Mierle, and Others. Ceres solver. <http://ceres-solver.org>. 1, 2, 7, 11
- [6] Sameer Agarwal, Noah Snavely, Steven M Seitz, and Richard Szeliski. Bundle adjustment in the large. In *European conference on computer vision*, pages 29–42. Springer, 2010. 1, 2, 3, 6, 11
- [7] Stephen Boyd, Neal Parikh, and Eric Chu. *Distributed optimization and statistical learning via the alternating direction method of multipliers*. Now Publishers Inc, 2011. 1
- [8] Xiaozhi Chen, Huimin Ma, Ji Wan, Bo Li, and Tian Xia. Multi-view 3d object detection network for autonomous driving. In *Proceedings of the IEEE conference on Computer Vision and Pattern Recognition*, pages 1907–1915, 2017. 1
- [9] Yanqing Chen, Timothy A Davis, William W Hager, and Sivasankaran Rajamanickam. Algorithm 887: Cholmod, supernodal sparse cholesky factorization and update/downdate. *ACM Transactions on Mathematical Software (TOMS)*, 35(3):1–14, 2008. 1, 6
- [10] Jeffrey Dean and Sanjay Ghemawat. Mapreduce: simplified data processing on large clusters. *Communications of the ACM*, 51(1):107–113, 2008. 5
- [11] Frank Dellaert and et al. Gtsam. <https://github.com/borglab/gtsam>, 2011. 2
- [12] Nikolaus Demmel, Maolin Gao, Emanuel Laude, Tao Wu, and Daniel Cremers. Distributed photometric bundle adjustment. In *2020 International Conference on 3D Vision (3DV)*, pages 140–149. IEEE, 2020. 1, 2
- [13] Nikolaus Demmel, Christiane Sommer, Daniel Cremers, and Vladyslav Usenko. Square root bundle adjustment for large-scale reconstruction. In *Proceedings of the IEEE/CVF Conference on Computer Vision and Pattern Recognition*, pages 11723–11732, 2021. 2, 11
- [14] Stanley C Eisenstat. Efficient implementation of a class of preconditioned conjugate gradient methods. *SIAM Journal on Scientific and Statistical Computing*, 2(1):1–4, 1981. 1
- [15] Athena Elafrou, Georgios I. Goumas, and Nectarios Koziris. A lightweight optimization selection method for sparse matrix-vector multiplication. *CoRR*, abs/1511.02494, 2015. 3
- [16] Anders Eriksson, John Bastian, Tat-Jun Chin, and Mats Isaksson. A consensus-based framework for distributed bundle adjustment. In *Proceedings of the IEEE Conference on Computer Vision and Pattern Recognition*, pages 1754–1762, 2016. 1
- [17] TJ Fountain. A review of simd architectures. *Image Processing System Architectures*, pages 3–22, 1985. 2
- [18] Marco Fratarcangeli, Derek Bradley, Aurel Gruber, Gaspard Zoss, and Thabo Beeler. Fast nonlinear least squares optimization of large-scale semi-sparse problems. In *Computer Graphics Forum*, volume 39, pages 247–259. Wiley Online Library, 2020. 2
- [19] Giorgio Grisetti, Rainer Kümmerle, Hauke Strasdat, and Kurt Konolige. g2o: A general framework for (hyper) graph optimization. In *Proceedings of the IEEE International Conference on Robotics and Automation (ICRA), Shanghai, China*, pages 9–13, 2011. 1, 2
- [20] Gaël Guennebaud, Benoît Jacob, et al. Eigen v3. <http://eigen.tuxfamily.org>, 2010. 6
- [21] Timo Hackel, Nikolay Savinov, Lubor Ladicky, Jan D Wegner, Konrad Schindler, and Marc Pollefeys. Semantic3d.net: A new large-scale point cloud classification benchmark. *arXiv preprint arXiv:1704.03847*, 2017. 1
- [22] Jingwei Huang, Shan Huang, and Mingwei Sun. Deeplm: Large-scale nonlinear least squares on deep learning frameworks using stochastic domain decomposition. In *Proceedings of the IEEE/CVF Conference on Computer Vision and Pattern Recognition*, pages 10308–10317, 2021. 1, 2, 7, 11
- [23] Sylvain Jaeger. Nccl 2.0. In *GPU Technology Conference (GTC)*, 2017. 2
- [24] Michael Kaess, Hordur Johannsson, Richard Roberts, Viorela Ila, John J Leonard, and Frank Dellaert. isam2: Incremental smoothing and mapping using the bayes tree. *The International Journal of Robotics Research*, 31(2):216–235, 2012. 2
- [25] Michael Kaess, Ananth Ranganathan, and Frank Dellaert. isam: Incremental smoothing and mapping. *IEEE Transactions on Robotics*, 24(6):1365–1378, 2008. 2
- [26] Kurt Konolige and Motilal Agrawal. Frameslam: From bundle adjustment to real-time visual mapping. *IEEE Transactions on Robotics*, 24(5):1066–1077, 2008. 1
- [27] Jesse Levinson, Jake Askeland, Jan Becker, Jennifer Dolson, David Held, Soeren Kammel, J Zico Kolter, Dirk Langer, Oliver Pink, Vaughan Pratt, et al. Towards fully autonomous driving: Systems and algorithms. In *2011 IEEE intelligent vehicles symposium (IV)*, pages 163–168. IEEE, 2011. 1
- [28] Peiliang Li, Xiaozhi Chen, and Shaojie Shen. Stereo r-cnn based 3d object detection for autonomous driving. In *Proceedings of the IEEE/CVF Conference on Computer Vision and Pattern Recognition*, pages 7644–7652, 2019. 1
- [29] Haomin Liu, Mingyu Chen, Guofeng Zhang, Hujun Bao, and Yingze Bao. Ice-ba: Incremental, consistent and efficient bundle adjustment for visual-inertial slam. In *Proceedings of the IEEE Conference on Computer Vision and Pattern Recognition*, pages 1974–1982, 2018. 2
- [30] Xinzhu Ma, Zhihui Wang, Haojie Li, Pengbo Zhang, Wanli Ouyang, and Xin Fan. Accurate monocular 3d object detection via color-embedded 3d reconstruction for autonomous driving. In *Proceedings of the IEEE/CVF International Conference on Computer Vision*, pages 6851–6860, 2019. 1
- [31] Donald W Marquardt. An algorithm for least-squares estimation of nonlinear parameters. *Journal of the society for Industrial and Applied Mathematics*, 11(2):431–441, 1963. 1

- [32] Helmut Mayer. RpbA – robust parallel bundle adjustment based on covariance information, 2019. [1](#), [2](#)
- [33] NVIDIA. Cusolver. <https://developer.nvidia.com/cusolver>. [6](#)
- [34] NVIDIA. Cusparse. <https://developer.nvidia.com/cusparse>. [6](#)
- [35] Joseph Ortiz, Mark Pupilli, Stefan Leutenegger, and Andrew J Davison. Bundle adjustment on a graph processor. In *Proceedings of the IEEE/CVF Conference on Computer Vision and Pattern Recognition*, pages 2416–2425, 2020. [2](#)
- [36] Youngmin Park, Vincent Lepetit, and Woontack Woo. Multiple 3d object tracking for augmented reality. In *2008 7th IEEE/ACM International Symposium on Mixed and Augmented Reality*, pages 117–120. IEEE, 2008. [1](#)
- [37] Michael JD Powell. A hybrid method for nonlinear equations. *Numerical methods for nonlinear algebraic equations*, 1970. [1](#)
- [38] Johannes Lutz Schönberger and Jan-Michael Frahm. Structure-from-motion revisited. In *Conference on Computer Vision and Pattern Recognition (CVPR)*, 2016. [11](#)
- [39] Johannes Lutz Schönberger, Enliang Zheng, Marc Pollefeys, and Jan-Michael Frahm. Pixelwise view selection for unstructured multi-view stereo. In *European Conference on Computer Vision (ECCV)*, 2016. [11](#)
- [40] Chengzhou Tang and Ping Tan. Ba-net: Dense bundle adjustment network. *arXiv preprint arXiv:1806.04807*, 2018. [2](#)
- [41] Bill Triggs, Philip F McLauchlan, Richard I Hartley, and Andrew W Fitzgibbon. Bundle adjustment—a modern synthesis. In *International workshop on vision algorithms*, pages 298–372. Springer, 1999. [1](#), [3](#)
- [42] Minh Vo, Srinivasa G Narasimhan, and Yaser Sheikh. Spatiotemporal bundle adjustment for dynamic 3d reconstruction. In *Proceedings of the IEEE Conference on Computer Vision and Pattern Recognition*, pages 1710–1718, 2016. [1](#)
- [43] Hao-Ren Wang, Juan Lei, Ao Li, and Yi-Hong Wu. A geometry-based point cloud reduction method for mobile augmented reality system. *Journal of Computer Science and Technology*, 33(6):1164–1177, 2018. [1](#)
- [44] Xipeng Wang, Ryan Marcotte, Gonzalo Ferrer, and Edwin Olson. Apriisam: Real-time smoothing and mapping. In *2018 IEEE International Conference on Robotics and Automation (ICRA)*, pages 2486–2493. IEEE, 2018. [2](#)
- [45] Robert WM Wedderburn. Quasi-likelihood functions, generalized linear models, and the gauss—newton method. *Biometrika*, 61(3):439–447, 1974. [1](#)
- [46] Changchang Wu, Sameer Agarwal, Brian Curless, and Steven M Seitz. Multicore bundle adjustment. In *CVPR 2011*, pages 3057–3064. IEEE, 2011. [1](#), [2](#), [7](#)
- [47] Runze Zhang, Siyu Zhu, Tian Fang, and Long Quan. Distributed very large scale bundle adjustment by global camera consensus. In *Proceedings of the IEEE International Conference on Computer Vision*, pages 29–38, 2017. [1](#)
- [48] Yiqin Zhao and Tian Guo. Pointar: Efficient lighting estimation for mobile augmented reality. In *European Conference on Computer Vision*, pages 678–693. Springer, 2020. [1](#)
- [49] Lei Zhou, Zixin Luo, Mingmin Zhen, Tianwei Shen, Shiwei Li, Zhuofei Huang, Tian Fang, and Long Quan. Stochastic bundle adjustment for efficient and scalable 3d reconstruction. In *European Conference on Computer Vision*, pages 364–379. Springer, 2020. [1](#)
- [50] Lei Zhou, Zixin Luo, Mingmin Zhen, Tianwei Shen, Shiwei Li, Zhuofei Huang, Tian Fang, and Long Quan. Stochastic bundle adjustment for efficient and scalable 3d reconstruction. In *European Conference on Computer Vision (ECCV)*, 2020. [1](#), [2](#), [7](#)

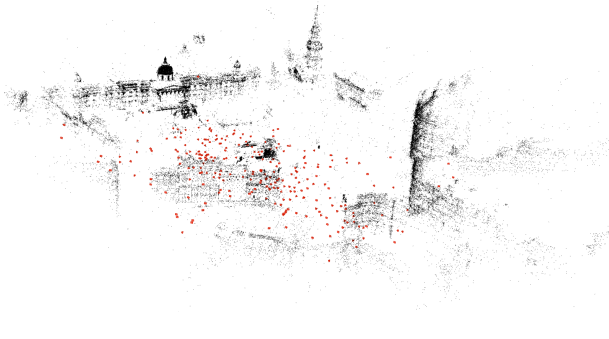
We provide additional experimental results on the whole BAL dataset [6] and their reconstruction plots. Refer to the Supplementary Material of [13] for the Problem sizes table.

A. Reconstruction Plots

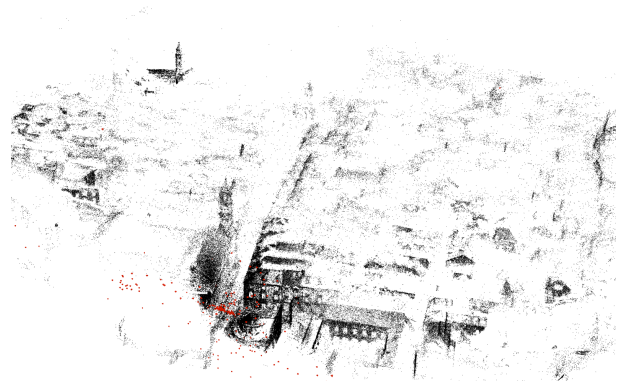
In this section, we show the optimized landmark point clouds (i.e. black dots) with cameras (i.e. red frames) for each dataset. The point clouds are rendered by COLMAP [38] [39].



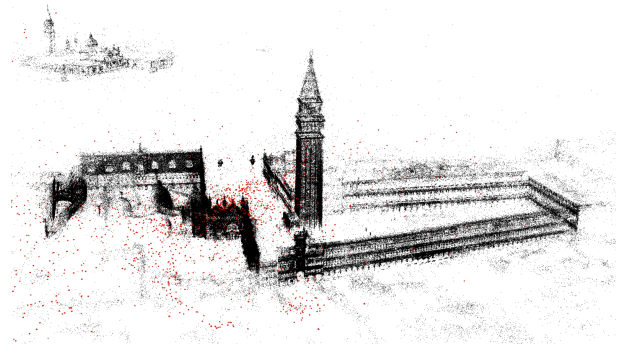
Ladybug



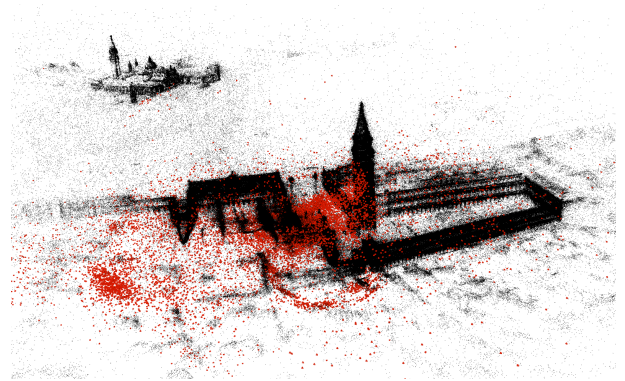
Trafalgar Square



Dubrovnik



Venice



Final

B. Experimental Results

We report MegBA (FP64, 1 GPU) compared with Ceres (16 threads) [5] and DeepLM (Ours-B setting) [22]. In the following tables, the columns *MegBA vs Ceres* and *MegBA vs DeepLM* indicate how much speedup MegBA outperforms Ceres and DeepLM, respectively.

For MegBA here, we implement a Levenberg–Marquardt algorithm with trust-region, according to [5]. Refer to our code for more details. Empirically, the choices of hyperparameters of the Levenberg–Marquardt algorithm would influence the convergence behavior (i.e. time and final

Mean Squared Error). We strongly suggest the practitioners to tune the parameters or develop customized trust-region strategies, when implementing MegBA with own projects.

	Ceres		DeepLM		MegBA		MegBA vs Ceres	MegBA vs DeepLM
	MSE	Time	MSE	Time	MSE	Time		
Ladybug-49	0.42	1.07	0.42	2.23	0.44	0.06	18.77×	39.07×
Ladybug-73	0.37	1.24	0.37	2.72	0.37	0.08	15.90×	34.85×
Ladybug-138	0.70	2.72	0.70	3.00	0.72	0.09	28.94×	31.96×
Ladybug-318	0.48	3.04	0.48	2.95	0.48	0.12	25.98×	25.18×
Ladybug-372	0.55	4.45	0.55	2.10	0.56	0.13	35.60×	16.80×
Ladybug-412	0.50	4.07	0.50	3.34	0.50	0.14	29.93×	24.57×
Ladybug-460	0.53	6.02	0.53	3.47	0.53	0.26	23.52×	13.56×
Ladybug-539	0.55	8.37	0.55	3.85	0.55	0.19	44.05×	20.25×
Ladybug-598	0.55	8.54	0.55	3.34	0.56	0.15	58.10×	22.75×
Ladybug-646	0.55	9.21	0.55	3.56	0.55	0.24	38.22×	14.79×
Ladybug-707	0.57	15.30	0.56	4.48	0.56	0.42	36.69×	10.74×
Ladybug-783	0.53	7.69	0.53	5.01	0.53	0.34	22.96×	14.95×
Ladybug-810	0.52	9.67	0.52	4.77	0.52	0.36	26.79×	13.22×
Ladybug-856	0.51	13.30	0.51	4.81	0.51	0.38	35.47×	12.83×
Ladybug-885	0.51	15.00	0.51	5.08	0.51	0.41	36.67×	12.42×
Ladybug-931	0.55	15.30	0.55	4.56	0.55	0.38	40.69×	12.14×
Ladybug-969	0.55	17.50	0.54	5.21	0.54	0.40	44.08×	13.14×
Ladybug-1031	0.55	12.90	0.55	4.04	0.55	0.63	20.64×	6.46×
Ladybug-1064	0.55	15.40	0.56	3.17	0.55	0.50	31.11×	6.40×
Ladybug-1118	0.57	15.40	0.58	3.68	0.57	1.21	12.69×	3.03×
Ladybug-1152	0.56	13.70	0.56	3.07	0.57	0.70	19.66×	4.40×
Ladybug-1197	0.57	17.30	0.57	4.13	0.57	0.74	23.32×	5.56×
Ladybug-1235	0.56	20.30	0.58	3.34	0.56	0.94	21.55×	3.55×
Ladybug-1266	0.57	23.60	0.56	4.53	0.56	0.91	26.02×	5.00×
Ladybug-1340	0.57	26.20	0.57	4.54	0.57	1.17	22.45×	3.89×
Ladybug-1469	0.56	26.30	0.57	3.84	0.57	0.91	28.90×	4.22×
Ladybug-1514	0.56	25.20	0.56	4.69	0.56	0.87	28.97×	5.39×
Ladybug-1587	0.59	37.50	0.56	4.82	0.57	0.90	41.90×	5.39×
Ladybug-1642	0.58	36.10	0.56	3.64	0.58	0.74	48.65×	4.91×
Ladybug-1695	0.56	32.30	0.56	4.24	0.56	1.10	29.42×	3.86×
Ladybug-1723	0.56	34.50	0.56	3.89	0.57	0.90	38.46×	4.34×

Table 5. Ladybug

	Ceres		DeepLM		MegBA		MegBA vs Ceres	MegBA vs DeepLM
	MSE	Time	MSE	Time	MSE	Time		
Trafalgar-21	0.83	0.42	0.83	1.72	0.83	0.58	0.74×	2.99×
Trafalgar-39	0.95	1.02	0.95	2.63	0.95	0.82	1.25×	3.22×
Trafalgar-50	0.70	1.04	0.70	2.62	0.70	1.18	0.88×	2.22×
Trafalgar-126	0.62	3.36	0.62	3.98	0.63	2.11	1.59×	1.89×
Trafalgar-138	0.53	8.11	0.53	4.00	0.53	3.35	2.42×	1.19×
Trafalgar-161	0.47	4.76	0.47	4.11	0.47	3.26	1.46×	1.26×
Trafalgar-170	0.47	6.77	0.47	4.00	0.47	3.35	2.02×	1.19×
Trafalgar-174	0.47	5.63	0.46	4.17	0.47	1.15	4.90×	3.63×
Trafalgar-193	0.46	7.13	0.46	4.17	0.47	1.22	5.83×	3.41×
Trafalgar-201	0.48	2.83	0.46	3.72	0.47	1.31	2.16×	2.84×
Trafalgar-206	0.45	12.80	0.45	4.36	0.46	0.68	18.77×	6.39×
Trafalgar-215	0.45	9.97	0.45	4.33	0.46	1.45	6.88×	2.99×
Trafalgar-225	0.44	5.55	0.44	4.49	0.45	1.67	3.33×	2.69×
Trafalgar-257	0.44	5.52	0.43	4.61	0.44	1.29	4.28×	3.58×

Table 6. Trafalgar

	Ceres		DeepLM		MegBA		MegBA vs Ceres	MegBA vs DeepLM
	MSE	Time	MSE	Time	MSE	Time		
Trafalgar-21	0.83	0.42	0.83	1.72	0.83	0.58	0.74×	2.99×
Trafalgar-39	0.95	1.02	0.95	2.63	0.95	0.82	1.25×	3.22×
Trafalgar-50	0.70	1.04	0.70	2.62	0.70	1.18	0.88×	2.22×
Trafalgar-126	0.62	3.36	0.62	3.98	0.63	2.11	1.59×	1.89×
Trafalgar-138	0.53	8.11	0.53	4.00	0.53	3.35	2.42×	1.19×
Trafalgar-161	0.47	4.76	0.47	4.11	0.47	3.26	1.46×	1.26×
Trafalgar-170	0.47	6.77	0.47	4.00	0.47	3.35	2.02×	1.19×
Trafalgar-174	0.47	5.63	0.46	4.17	0.47	1.15	4.90×	3.63×
Trafalgar-193	0.46	7.13	0.46	4.17	0.47	1.22	5.83×	3.41×
Trafalgar-201	0.48	2.83	0.46	3.72	0.47	1.31	2.16×	2.84×
Trafalgar-206	0.45	12.80	0.45	4.36	0.46	0.68	18.77×	6.39×
Trafalgar-215	0.45	9.97	0.45	4.33	0.46	1.45	6.88×	2.99×
Trafalgar-225	0.44	5.55	0.44	4.49	0.45	1.67	3.33×	2.69×
Trafalgar-257	0.44	5.52	0.43	4.61	0.44	1.29	4.28×	3.58×

Table 7. Trafalgar

	Ceres		DeepLM		MegBA		MegBA vs Ceres	MegBA vs DeepLM
	Error	Time	Error	Time	Error	Time		
Dubrovnik-16	0.22	0.79	0.22	1.75	0.22	1.56	0.50×	1.12×
Dubrovnik-88	0.75	7.69	0.75	4.77	0.75	0.93	8.23×	5.11×
Dubrovnik-135	0.67	17.00	0.67	5.88	0.68	1.11	15.30×	5.29×
Dubrovnik-142	0.48	17.30	0.48	6.03	0.49	1.32	13.14×	4.58×
Dubrovnik-150	0.43	15.20	0.43	6.27	0.44	0.94	16.20×	6.68×
Dubrovnik-161	0.41	16.80	0.41	7.61	0.41	0.76	22.08×	10.01×
Dubrovnik-173	0.41	15.40	0.41	7.38	0.41	0.80	19.20×	9.21×
Dubrovnik-182	0.45	13.40	0.45	8.11	0.46	1.01	13.28×	8.04×
Dubrovnik-202	0.43	21.70	0.43	9.40	0.44	0.98	22.08×	9.56×
Dubrovnik-237	0.42	25.50	0.42	9.95	0.41	1.27	20.02×	7.81×
Dubrovnik-253	0.38	29.00	0.38	10.82	0.39	1.08	26.80×	10.00×
Dubrovnik-262	0.37	95.90	0.37	11.25	0.38	1.17	82.18×	9.64×
Dubrovnik-273	0.37	47.90	0.37	11.41	0.37	0.91	52.70×	12.55×
Dubrovnik-287	0.36	26.80	0.36	11.43	0.37	0.98	27.49×	11.72×
Dubrovnik-308	0.37	33.80	0.37	11.22	0.38	1.27	26.53×	8.81×
Dubrovnik-356	0.39	116.00	0.39	14.05	0.41	1.68	68.92×	8.35×

Table 8. Dubrovnik

	Ceres		DeepLM		MegBA		MegBA vs Ceres	MegBA vs DeepLM
	MSE	Time	MSE	Time	MSE	Time		
Venice-52	0.75	7.95	0.75	4.66	0.79	1.64	4.86×	2.85×
Venice-89	0.50	8.47	0.50	6.41	0.50	6.38	1.33×	1.00×
Venice-245	0.84	31.90	0.87	5.66	0.83	10.64	3.00×	0.53×
Venice-427	0.63	58.20	0.63	15.46	0.62	6.97	8.35×	2.22×
Venice-744	0.51	109.00	0.51	27.79	0.51	5.48	19.88×	5.07×
Venice-951	0.44	84.30	F	F	0.48	6.98	12.07×	N/A
Venice-1102	0.40	146.00	0.39	32.80	0.39	13.69	10.67×	2.40×
Venice-1158	0.42	33.10	0.43	12.07	0.47	5.08	6.52×	2.38×
Venice-1184	0.74	42.70	0.35	36.32	0.34	36.24	1.18×	1.00×
Venice-1238	0.35	71.40	0.34	13.20	0.35	5.24	13.63×	2.52×
Venice-1288	0.33	153.00	0.33	19.79	0.33	16.97	9.01×	1.17×
Venice-1350	0.34	52.30	0.34	10.47	0.33	6.85	7.64×	1.53×
Venice-1408	0.35	76.50	0.35	10.72	0.34	5.60	13.66×	1.91×
Venice-1425	0.34	153.00	0.34	10.80	0.34	6.88	22.23×	1.57×
Venice-1473	0.33	110.00	0.33	43.24	0.33	5.58	19.73×	7.76×
Venice-1490	0.33	66.80	0.33	14.25	0.32	5.66	11.80×	2.52×
Venice-1521	0.33	75.60	0.33	10.98	0.33	5.76	13.14×	1.91×
Venice-1544	0.33	173.00	0.33	26.59	0.32	5.70	30.37×	4.67×
Venice-1638	0.57	75.40	0.58	30.04	0.59	25.37	2.97×	1.18×
Venice-1666	0.48	74.00	0.48	23.48	0.51	7.17	10.33×	3.28×
Venice-1672	0.38	260.00	0.38	33.49	0.43	8.53	30.49×	3.93×
Venice-1681	0.37	48.40	0.34	46.98	0.36	8.83	5.48×	5.32×
Venice-1682	0.34	164.00	0.33	38.92	0.35	8.73	18.78×	4.46×
Venice-1684	0.34	207.00	0.33	43.94	0.35	8.87	23.33×	4.95×
Venice-1695	0.37	53.40	0.34	44.99	0.36	8.70	6.14×	5.17×
Venice-1696	0.38	43.00	0.33	47.04	0.34	7.14	6.02×	6.58×
Venice-1706	0.34	234.00	0.34	38.17	0.36	5.76	40.60×	6.62×
Venice-1776	0.33	192.00	0.33	46.69	0.33	7.32	26.22×	6.38×
Venice-1778	0.33	403.00	0.33	46.16	0.33	7.28	55.34×	6.34×

Table 9. Venice, F stands for failed

	Ceres		DeepLM		MegBA		MegBA vs Ceres	MegBA vs DeepLM
	MSE	Time	MSE	Time	MSE	Time		
Final-93	0.51	4.10	0.51	1.56	0.51	1.48	2.77×	1.05×
Final-394	0.56	30.10	0.56	5.10	0.56	1.70	17.69×	3.00×
Final-871	0.62	115.00	0.62	26.12	0.63	3.45	33.34×	7.57×
Final-961	0.94	44.30	0.94	12.82	0.94	1.10	40.46×	11.70×
Final-1936	0.89	106.00	0.89	17.03	0.89	4.17	25.44×	4.09×
Final-3068	1.09	31.60	1.03	5.49	1.13	2.39	13.25×	2.30×
Final-4585	0.57	417.00	0.56	66.13	0.57	11.85	35.20×	5.58×

Table 10. Final